Optimal Energy Storage Sizing and Control for Wind Power Applications

Ted K. A. Brekken, *Member, IEEE*, Alex Yokochi, Annette von Jouanne, *Fellow, IEEE*, Zuan Z. Yen, Hannes Max Hapke, *Member, IEEE*, and Douglas A. Halamay, *Student Member, IEEE*

***Abstract*—The variable output of a large wind farm presents many integration challenges, especially at high levels of penetration. The uncertainty in the output of a large wind plant can be covered by using fast-acting dispatchable sources, such as natural gas turbines or hydro generators. However, using dispatchable sources on short notice to smooth the variability of wind power can increase the cost of large-scale wind power integration. To remedy this, the inclusion of large-scale energy storage at the wind farm output can be used to improve the predictability of wind power and reduce the need for load following and regulation hydro or fossil-fuel reserve generation. This paper presents sizing and control methodologies for a zinc–bromine flow battery-based energy storage system. The results show that the power flow control strategy does have a significant impact on proper sizing of the rated power and energy of the system. In particular, artificial neural network control strategies resulted in significantly lower cost energy storage systems than simplified controllers. The results show that through more effective control and coordination of energy storage systems, the predictability of wind plant outputs can be increased and the cost of integration associated with reserve requirements can be decreased.**

***Index Terms*—Control systems, energy storage, power generation dispatch, power system security, wind energy.**

NOMENCLATURE

Parameters and Variables

P_{rated}	Energy storage system rated power in per unit.
J_{rated}	Energy storage system rated energy capacity in per unit power hours.
T	Fraction of simulation samples in which the error in forecasted output is within the allowed band.
η	Energy storage one-way efficiency.

Time Series Data

P_{wind}	Wind farm output power.
$P_{\mathrm{wind,FC}}$	Forecasted wind farm output power.
$P_{\mathrm{ES,cmd}}$	Commanded energy storage power.
P_{ES}	Energy storage power.
P_{total}	Wind farm plus energy storage power output.
SOC	Energy storage state of charge.
$P_{\mathrm{wind,err}}$	Difference between forecasted output and wind farm output.
$P_{\mathrm{total,err}}$	Difference between forecasted output and wind farm plus energy storage output.

All power and energy are in per unit

I. INTRODUCTION

WIND energy has experienced phenomenal growth in the last 20 years. Recently, the United States became the world leader in installed wind power capacity. In the Pacific Northwest, it is predicted that as much as an additional 5000 MW of wind power could come online within the next five years [1]. The variable nature of a wind farm output presents many challenges for grid operators. The uncertainty in the output of a large wind plant can be covered by using fast-acting dispatchable sources, such as natural gas turbines or hydro generators. However, using dispatchable sources on short notice to smooth the variability of wind power can increase the cost of large-scale wind power integration through increased reserve requirements. In addition, using hydro generators to track demand, including covering for wind forecast imbalances, can result in greater maintenance requirements. This research is focused on an analysis of the feasibility of using large-scale energy storage to improve the predictability of a wind farm output. The goal of the energy storage system is to allow the combined output of a large wind farm and an on-site energy storage system to meet an hour-ahead predicted power output within $\pm 4\%$, 90% of the time [2].

There are two main objectives of the research.

1) Determine the lowest-cost flow-battery-based energy storage system for use in conjunction with a large wind farm that allows the combined wind plant and energy storage output to meet the forecasted wind farm output within $\pm 4\%$, 90% of the time.
2) Determine the effect of the energy storage power flow control strategy on sizing and system requirements.

The main contribution of this research is a methodology for sizing large-scale energy storage for wind farm applications, while also quantifying the impact of control strategy on sizing.

Manuscript received February 09, 2010; revised June 22, 2010; accepted August 05, 2010. Date of publication August 12, 2010; date of current version December 15, 2010. This work was supported by Bonneville Power Administration (BPA), by Central Lincoln PUD, and by Oregon BEST.

T. K. A. Brekken, A. Yokochi, A. von Jouanne, and D. A. Halamay are with the School of Electrical Engineering and Computer Science, Oregon State University, Corvallis, OR 97331 USA (e-mail: brekken@eecs.oregonstate.edu).

Z. Z. Yen was with Oregon State University, Corvallis, OR 97331 USA. He is now with the U.S. Army Corps of Engineers, Portland, OR 97209-4141 USA.

H. M. Hapke was with Oregon State University, Corvallis, OR 97331 USA. He is now with Vestas, Aarhus 8200, Denmark.

Color versions of one or more of the figures in this paper are available online at http://ieeexplore.ieee.org.

Digital Object Identifier 10.1109/TSTE.2010.2066294

II. Background

The goal of using an energy storage system in conjunction with a large wind farm is to allow the combined output to meet an hour-ahead predicted output within $\pm 4\%$, 90% of the time. This constraint is based on over or under production penalties specified by the Bonneville Power Administration (BPA) [2]. Details on the imbalance penalties are given in the Appendix.

A. Literature Review

In the literature, there is work being done on sizing of energy storage systems for use with combined stand-alone diesel and wind systems [3]–[5]. There are also investigations on the use of energy storage applied to a single wind turbine for buffering the variability of the output [6]–[8]. At the wind farm scale, research has been done on the effectiveness of battery energy storage for improving the variability of wind farm output. Publications [9] and [10] demonstrate the modeling and operation of energy storage for a 50- and 80-MW wind farm. Other research demonstrates the possibility of using NaS batteries for providing system stability in the case of large variations in wind farm output, such as sudden loss of generation [11], [12]. Publications [13] and [14] demonstrate optimal control for a generic battery energy storage system for use with large wind farms. This work is unique in focusing on control and sizing of zinc–bromine flow batteries for a large wind farm.

B. Energy Storage

The cost models used in this research are based on a zinc–bromine flow battery [15], [16]. This battery technology is well suited for large-scale energy storage applications due to high power and energy capability, scalability, fairly fast response time, simple maintenance requirements, and high cycle life [17]–[20].

Other forms of energy storage, such as supercapacitors and flywheels for very fast power quality control, and pumped-storage and compressed area for very long-term storage, are not considered in this research, but are promising areas for future investigation [8], [21], [22]. Hydrogen is an often considered storage medium, but results so far suggest the cost to be prohibitive due to the poor round-trip efficiency and low energy density [23].

As is the case with all battery systems, the zinc–bromine system suffers from system inefficiencies, with the main losses in this system stemming from the electrochemical deviation from the ideal battery cell potentials under current flow conditions and internal resistive losses due to mass transfer effects [24]. Since all of these losses are dependent on current density within the battery, the most straightforward manner to address these in a simple model is to assign a loss of 15% to the energy flowing into the battery and 15% to the energy flowing out of it for an average battery efficiency of 72.25% (0.85×0.85). This simplifies future refinements of the model that include current density dependent effects. A 15% energy loss is an approximation of the real world losses incurred by an energy storage device similar to a flow cell battery. Further characterization, including hardware testing, may yield a more complex efficiency model for use in future simulations.

C. Forecasting

The combined wind farm and energy storage output is forecasted using a one-hour ahead persistence model. A new forecast for the next hour is determined every 20 minutes before the top of the hour. This research uses actual wind farm data from a large modern wind farm over 282 days. The power data (P_{wind}) sample time is 10 minutes, where each sample is a 10-minute average of higher resolution data recorded on-site. The forecast for the previous hour to the next hour linearly transitions from 10 minutes before the hour to 10 minutes after the hour. An example is given below. At 1:40, 20 minutes before the top of the hour, the forecast for the six sample points 2:00 through 2:50 (at 10-minute intervals) is made. The forecasted power at the five sample points 2:10 through 2:50 is set as the actual measured power at 1:40, as shown in (1). The forecasted power for 2:00 is set as the midpoint between the forecasted power for 1:50 (which had been determined the previous hour at 12:40) and the newly determined forecasted power at 2:10, as shown in (2). This process is repeated every hour, 20 minutes before the top of the hour

$$\begin{aligned} &P_{\mathrm{wind,FC}}(2:10, 2:20, 2:30, 2:40, 2:50) \\ &\quad = P_{\mathrm{wind}}(1:40) \qquad (1) \\ &P_{\mathrm{wind,FC}}(2:00) = \mathrm{mean}\left(P_{\mathrm{wind,FC}}(1:50, 2:10)\right). \qquad (2) \end{aligned}$$

D. Simulation

All simulations and analysis are conducted using MATLAB. A block diagram of the simulation flow is shown in Fig. 1. The energy controller determines the desired energy storage power output at the current simulation instant, $P_{\mathrm{ES,cmd}}$, based on the energy storage state of charge, SOC, the forecasted output, $P_{\mathrm{wind,FC}}$ (i.e., the power the utility operator is expecting from the wind farm), and the actual wind farm output P_{wind}.

The energy storage system is made up of two main components: the power converter and the battery. The energy storage converter produces the commanded output power $P_{\mathrm{ES,cmd}}$, if the SOC is not at a limit, and the commanded power does not exceed the energy storage system rating P_{rated}. P_{rated} is to be optimized

$$P_{\mathrm{ES}} = \begin{cases} 0, & \mathrm{SOC} = 0 \;\; \& \;\; P_{\mathrm{ES,cmd}} > 0 \\ 0, & \mathrm{SOC} = 1 \;\; \& \;\; P_{\mathrm{ES,cmd}} < 0 \\ P_{\mathrm{rated}}, & P_{\mathrm{ES,cmd}} > P_{\mathrm{rated}} \;\; \& \;\; \mathrm{SOC} \neq 0 \\ -P_{\mathrm{rated}}, & P_{\mathrm{ES,cmd}} < -P_{\mathrm{rated}} \;\; \& \;\; \mathrm{SOC} \neq 1 \\ P_{\mathrm{ES,cmd}}, & \text{else.} \end{cases} \qquad (3)$$

Positive P_{ES} is defined as power sourced by the energy storage (discharging), and negative P_{ES} is power into the energy storage (charging). The energy storage battery block then updates the SOC as a function of the power into or out of the battery. The rated energy capacity J_{rated} is to be optimized

$$\mathrm{SOC} = \mathrm{SOC}_{-1} - \frac{\eta \cdot P_{\mathrm{ES},-1}}{6 \cdot J_{\mathrm{rated}}} \qquad (4)$$

$$\eta = \begin{cases} \eta_{\mathrm{out}}, & P_{\mathrm{ES},-1} > 0 \\ \eta_{\mathrm{in}}, & P_{\mathrm{ES},-1} < 0 \end{cases} \qquad (5)$$

$$0 \leq \mathrm{SOC} \leq 1. \qquad (6)$$

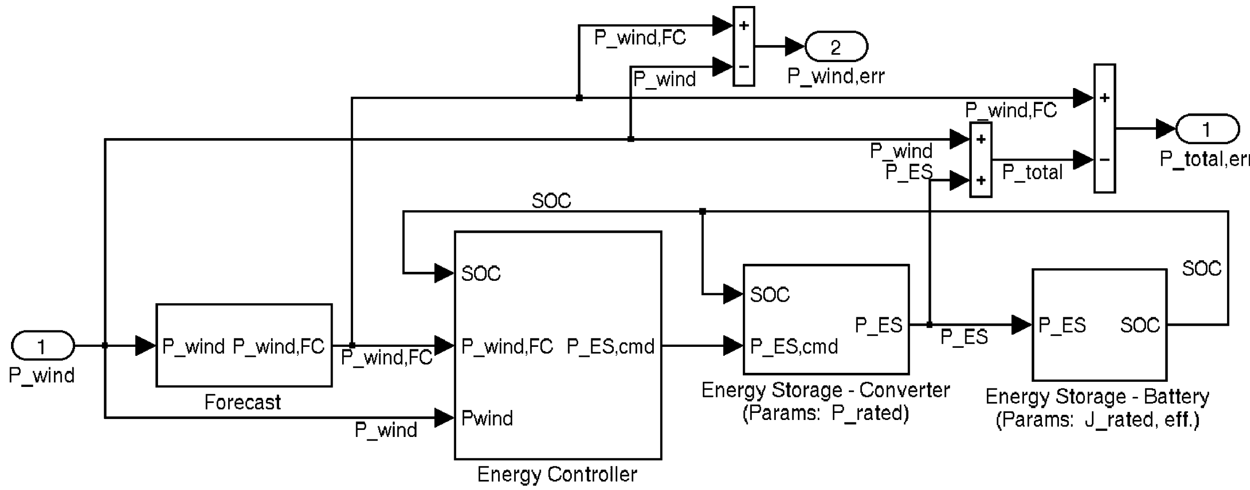

Fig. 1. Simulation block diagram.

The -1 subscript refers to the value at the previous sample. The 1/6 factor in (4) is due to the 10-minute sample time of the time series data and J_{rated} in units of per unit power hours. As described in Section II-B, η_{out} is 1.15 and η_{in} is 0.85. This will cause a 15% energy loss every time power is moved in or out of the energy storage battery.

The combined wind farm and energy storage output is $P_{\mathrm{wind}} + P_{\mathrm{ES}} = P_{\mathrm{total}}$, and the difference between the forecasted wind farm output and the actual combined output $P_{\mathrm{wind,FC}} - P_{\mathrm{total}} = P_{\mathrm{total,err}}$ is then the power that the utility must cover on short notice.

E. Cost Function

Following an extensive literature and equipment manufacturer cost search, a reasonable cost model for flow cell battery energy storage devices is defined as

$$\mathrm{Cost} = f(T) \cdot (C_P \cdot P_{\mathrm{rated}} + C_J \cdot J_{\mathrm{rated}}) \tag{7}$$

$$C_P = 0.20 \quad [\$/W] \tag{8}$$

$$C_J = 0.48 \quad [\$/Wh] \tag{9}$$

where P_{rated} is the rated power capability of the energy storage system and J_{rated} is the rated energy capacity of the system [2], [19], [20]. T is the fraction of samples in the simulation duration in which $P_{\mathrm{total,err}}$ is within of the desired ± 0.04 band. The term $f(T)$ is added to penalize energy storage systems in the solution space that do not meet the $|P_{\mathrm{total,err}}| \leq 0.04$ constraint

$$f(T) = \begin{cases} 1, & T \geq 0.9 \\ \infty, & T < 0.9. \end{cases} \tag{10}$$

III. Control Overview

Four energy storage control types are evaluated: simple, fuzzy, simple artificial neural network (ANN), and advanced ANN.

A. Simple

For the simple controller, the energy storage system is commanded to source or sink power equal to the error between the forecasted output of the wind farm and the actual power when the absolute error exceeds 0.04 per unit. The energy storage unit will not source power if the SOC is equal to 0, or sink power if the SOC is equal to 1. For the energy storage, positive power is defined as sourced power (i.e., power out). If the commanded power $P_{\mathrm{ES,cmd}}$ exceeds the rated power P_{rated}, the output power P_{ES} is saturated at the rated power.

- Input: $P_{\mathrm{wind,err}}$.
- Output: $P_{\mathrm{ES,cmd}}$

$$P_{\mathrm{ES,cmd}} = \begin{cases} P_{\mathrm{wind,err}}, & |P_{\mathrm{wind,err}}| > 0.04 \\ 0, & |P_{\mathrm{wind,err}}| \leq 0.04. \end{cases} \tag{11}$$

B. Fuzzy

Rather than explicitly covering the error in forecasted output as with the simple controller, the fuzzy controller commands the energy storage output with consideration of the magnitude of the error and the value of the SOC. The rules are given in Table I. For the error between forecasted wind farm output and actual output $P_{\mathrm{wind,err}}$, a "surplus" denotes there is more wind power than forecasted and $P_{\mathrm{wind,err}} < 0$. If the SOC is in the state of "discharged," it is an ideal situation for the energy storage system to accept energy and the commanded energy storage system power is equal to the power necessary to cover the error in forecasted power.

- Inputs: SOC, $P_{\mathrm{wind,err}}$.
- Output: $P_{\mathrm{ES,cmd}}$.

The memberships are triangular functions with the vertices given in Table II.

Note that even though some of the membership functions for SOC are specified out to infinity, the SOC is limited to $0 \leq \mathrm{SOC} \leq 1$.

C. Simple ANN

The third control method tested is a simple ANN. It is similar to the simple controller in that it does not consider the current SOC. ANNs may be advantageous in this application as they may be able to be trained to maximize the use of the energy storage system. There are examples of ANNs being used in other energy storage applications including microgrids and electric vehicles [25]–[28].

- Inputs: $P_{\mathrm{wind,FC}}$, P_{wind}.

TABLE I
FUZZY RULES

SOC	$P_{wind,err}$	$P_{ES,cmd}$
discharged	surplus	$P_{wind,err}$
discharged	accurate	0
discharged	deficit	0
medium charge	surplus	$P_{wind,err}$
medium charge	accurate	0
medium charge	deficit	$P_{wind,err}$
charged	surplus	0
charged	accurate	0
charged	deficit	$P_{wind,err}$

TABLE II
FUZZY MEMBERSHIPS

Variable	Set	Tri. Membership Vertices
SOC	discharged	($-\infty$, 0, 0.2)
SOC	medium charge	(0.2, 0.5, 0.8)
SOC	charged	(0.8, 1, ∞)
$P_{wind,err}$	deficit	(0, 0.04, ∞)
$P_{wind,err}$	accurate	(-0.04, 0, 0.04)
$P_{wind,err}$	surplus	($-\infty$, -0.04, 0)

- Output: $P_{\mathrm{ES,cmd}}$.
- Three layers: 2 input neurons, 2 hidden neurons, 1 output neuron.
- Bipolar sigmoid hidden layer activation function and linear output layer activation function.

The ANN is trained using a genetic algorithm. The cost function (i.e., fitness function) for evaluation and training is (7). Details of the training are given in Section IV-C.

D. Advanced ANN

The advanced version of the neural network has an additional input and more hidden neurons.

- Inputs: $P_{\mathrm{wind,FC}}$, P_{wind}, SOC.
- Output: $P_{\mathrm{ES,cmd}}$.
- Three layers: 3 input neurons, 3 hidden neurons, 1 output neuron.
- Bipolar sigmoid hidden layer activation function and linear output layer activation function.

As with the simple case, the advanced ANN is trained with a genetic algorithm. The cost function (i.e., fitness function) for evaluation and training is (7).

IV. Optimization Methodology

A. Performance Evaluation by Simulation

The performance of a given control method, energy storage power rating (P_{rated}), and energy storage energy capacity rating (J_{rated}) is evaluated by running a full simulation of the combined system shown in Fig. 1 over a full 282 days of wind power data.

Figs. 2 and 3 show time domain results of a single simulation result with $P_{\mathrm{rated}} = 0.340$, $J_{\mathrm{rated}} = 0.400$, and the simple energy storage power control scheme. After the simulation is complete, the time series data is analyzed to determine T, the fraction of samples in which $|P_{\mathrm{total,err}}| \leq 0.04$. The rated power, rated energy, and T are then used to calculate the cost function, as shown in (7). Other statistics on $P_{\mathrm{total,err}}$ are also calculated, including mean absolute error (MAE), RMS error (RMSE), maximum error, minimum error, and standard deviation.

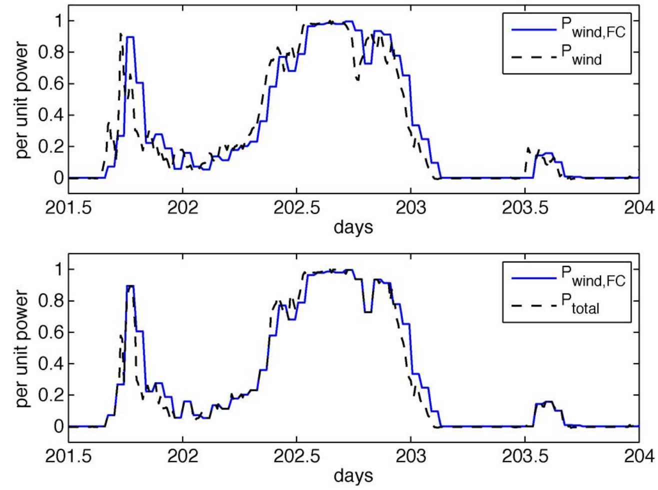

Fig. 2. Forecasted wind power, actual wind power, and total system power.

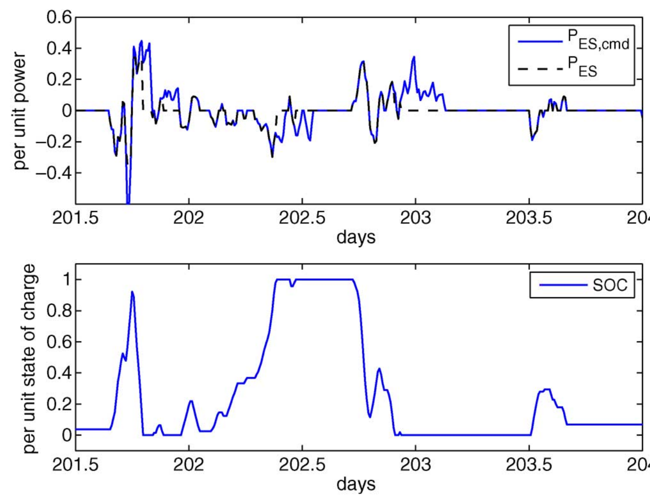

Fig. 3. Energy storage power and state of charge.

Actual energy price data at a nearby trading hub has also been obtained over the 282 day period of real wind power data. The price data is used to calculate the total revenue, as well as penalty costs incurred from failing to meet the forecasted power. Note that this penalty cost and revenue is not used in the cost function for optimization. It is presented in the results as a point of interest, and could be used in future optimizations. Details on the calculation of the penalty cost due to imbalance are given in the Appendix.

Fig. 4 shows the histogram of the error between the forecasted wind farm power and the actual wind farm power $P_{\mathrm{wind,err}}$, and the error between the forecasted wind farm power and the combined farm and energy storage power $P_{\mathrm{total,err}}$. It can be

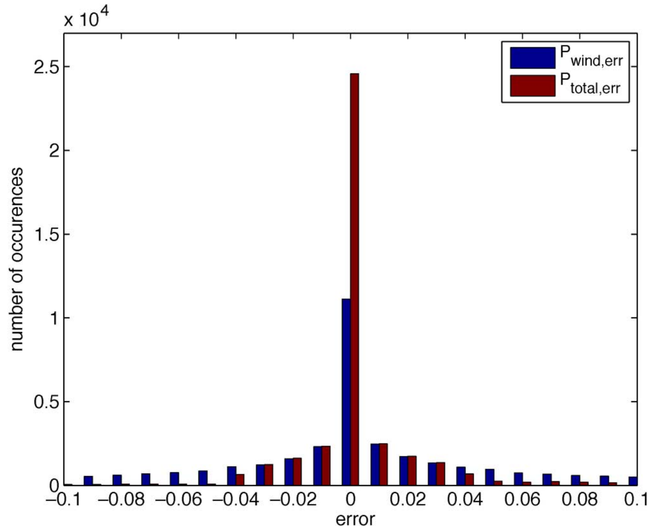

Fig. 4. Histogram of $P_{\text{wind,err}}$ and $P_{\text{total,err}}$.

seen that there are many more occurrences of 0 for $P_{\text{total,err}}$, and that errors toward the wings of the distribution for $P_{\text{wind,err}}$ have been moved to 0 for $P_{\text{total,err}}$. This clearly shows the effect of the energy storage system as outlier errors beyond the ± 0.04 band are moved to 0 error, thus demonstrating that the energy storage system allows the combined wind farm and energy storage output to match the forecasted output with much greater reliability.

B. Simple and Fuzzy Controllers

For the simple controller and fuzzy controller, determination of the optimal P_{rated} and J_{rated} was done by a simple linear search. The procedure is given below:

1) Choose controller type (e.g., simple or fuzzy).
2) Initialize P_{rated} and J_{rated} with starting values.
3) Run one simulation on entire wind farm power data set (282 days).
4) Calculate T, the fraction of sample points in which $|P_{\text{total,err}}| \le 0.04$.
5) Calculate cost $\text{Cost}(T, P_{\text{rated}}, J_{\text{rated}})$.
6) Calculate other metrics, including $P_{\text{total,err}}$ statistics and revenue and imbalance penalties.
7) Increment P_{rated} and return to 3) until final P_{rated} value reached.
8) Increment J_{rated} and return to 3) until final J_{rated} value reached.

This procedure then yields the lowest cost system that meets the desired constraints. Fig. 5 shows T, the fraction of sample points for which $|P_{\text{total,err}}| \le 0.04$, for each combination of P_{rated} and J_{rated} using the simple controller. Fig. 6 shows the corresponding costs for each system after the cost surface has been masked by all systems for which $T \ge 0.9$. For illustration, the lowest cost system has been annotated on the figures.

The same methodology is applied to the fuzzy controller. The corresponding results are shown in Figs. 7 and 8.

Note that for the examples shown, the resolution in the search is relatively low: 0.1 steps in P_{rated} and J_{rated}. After the low resolution search, the search is repeated at a resolution of 0.01 around the low resolution solution. The results of the high resolution search are given in Section V.

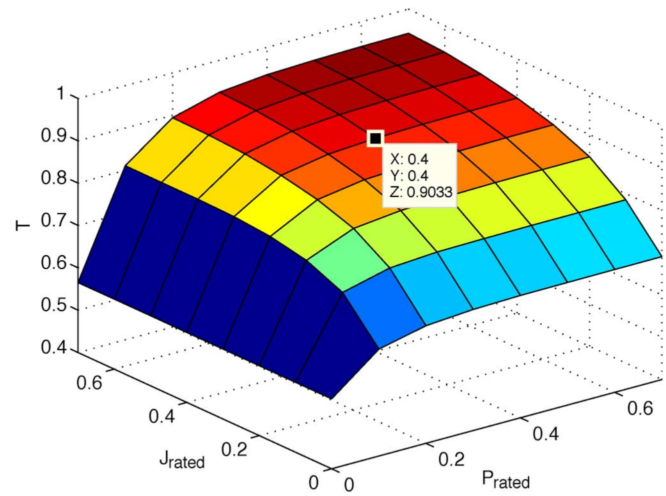

Fig. 5. T surface for simple controller.

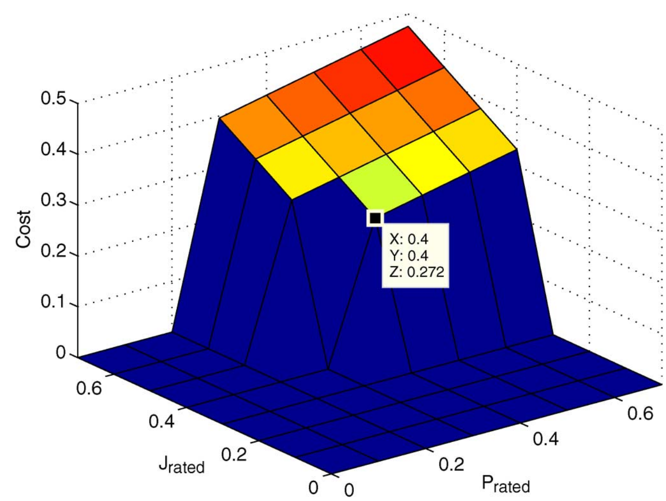

Fig. 6. Cost surface for simple controller.

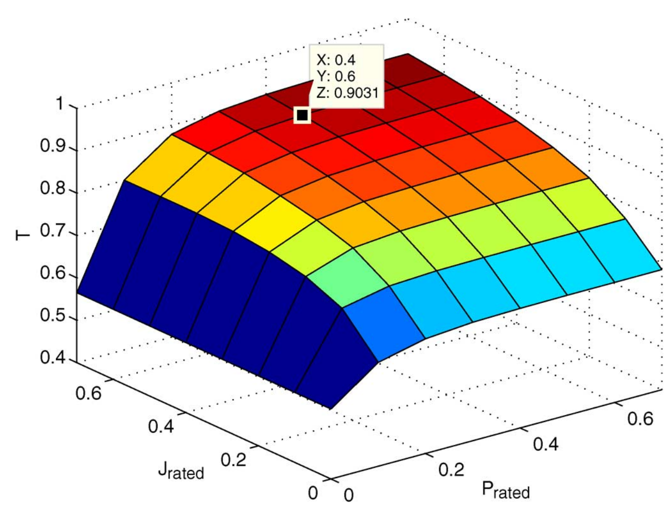

Fig. 7. T surface for fuzzy controller.

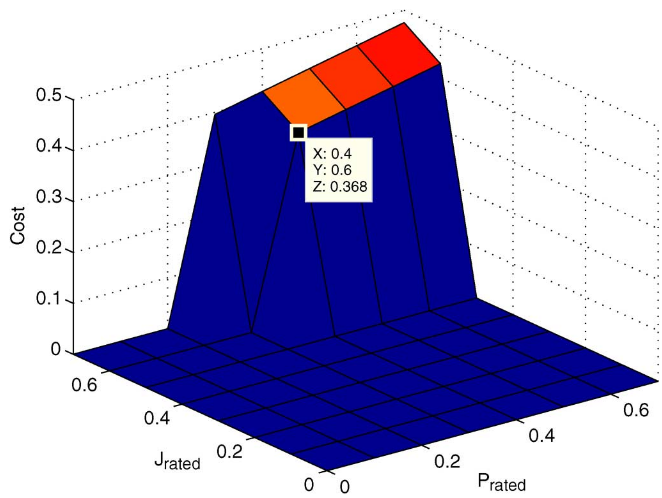

Fig. 8. Cost surface for fuzzy controller.

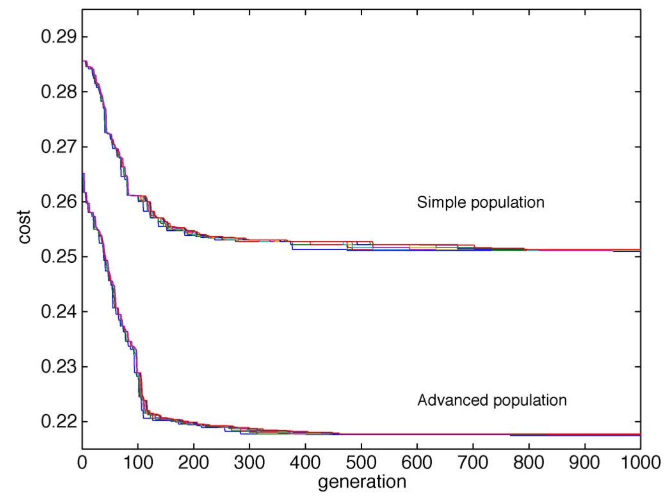

Fig. 9. Population cost history for training of simple and advanced ANNs.

C. ANN Controllers

For the simple and advanced variations of the ANN controllers, a genetic algorithm based unsupervised training method was used to optimize both the energy storage parameters (P_{rated} and J_{rated}) and the ANN weights together. The chromosome is of the form

$$[P_{\text{rated}} \quad J_{\text{rated}} \quad w_1 \quad w_2 \quad w_3 \quad \ldots] \tag{12}$$

where $w_1, w_2, w_3, \ldots$ are the weights between the neuron layers. The activation function bias is accounted for in the weights as a weight between any neuron input and a constant of value 1 [29], [30]. The difference between the simple and advanced variation is in the number of inputs and the number of hidden neurons, as explained in Section III. The genetic algorithm optimization procedure is as follows:

1) Choose controller type (e.g., simple or advanced).
2) Initialize random population of 20 members, each with a chromosome as given in (12).
3) For each member of the population:
   a) Run one simulation on one month of P_{wind}.
   b) Calculate T, the fraction of sample points in which $|P_{\text{total,err}}| \leq 0.04$.
   c) Calculate the cost (i.e., fitness) function Cost [see (7)].
4) Cull the 10 members of the population with the highest Cost.
5) Randomize the order of the remaining 10 and split into two parent groups.
6) Clone each parent group to produce two child groups.
7) Randomly cross (i.e., swap) genes between corresponding gene positions between the two child groups.
8) Combine the two child groups into one child group.
9) Randomly mutate the genes in the child group by adding a random offset to genes and multiplying by a random factor.
10) Append the child group to the parent group and return to 3) until 1000 generations has been reached.
11) Save ANN weights P_{rated} and J_{rated} of the highest performing population member (i.e., lowest Cost).

The genetic algorithm is set up such that the cross (i.e., swap) rate starts high for the first generations and decreases for each generation iteration. The cross rate starts at 50% and decreases to 10% by the final generation. Conversely, the mutation rate is set low to start with and increases as the algorithm progresses. It starts at 10% and increases to 50%. It was found that seeding the initial randomized population with a P_{rated} and J_{rated} from the earlier linear optimizations greatly decreased the convergence time. Thus, the algorithm is biased toward gene crossing early on to allow the seeded member to propagate its genes, and then switching focus to mutation toward the end to make modifications to high performing members.

Fig. 9 shows the cost of the 10 members of both the simple population and the advanced population versus generation. By the 1000th generation, the populations were tightly grouped with the most fit member of the simple population at a cost of 0.251, and the most fit member of the advanced population at a cost of 0.218.

V. Optimization Results

A summary of the results is given in Table III and Fig. 10. Table III shows the resulting optimized system for each control strategy. Cost is given in \$/W. For example, for a 100-MW wind farm using the simple control scheme for the energy storage system, the minimum cost system is rated for 34 MW and 40 MWh, and costs \$26 million. MAE, RMSE, max(E), and min(E) are the mean absolute error, root mean squared error, maximum error, and minimum error of $P_{\text{wind,FC}} - P_{\text{total}} = P_{\text{total,err}}$, respectively. As discussed in Section IV-A, an additional set of cost and revenue metrics were calculated. R_{base} is the base revenue of the combined wind farm and energy storage system in energy sales in \$/W/yr, before imbalanced penalties are applied. C_{pen} is the cost of any occurrences of failing to meet the forecasted power (i.e., $|P_{\text{total,err}}| > 0.04$) and is subtracted from R_{base} to give the total revenue R_{total}. Details on the calculation of revenue and imbalance cost are given in the Appendix. The revenue and costs were calculated over the simulation length, 282 days, and scaled by 365/282 to be expressed per year.

Fig. 10 shows a histogram of the error in forecasted output and combined wind farm and energy storage output $(P_{\text{total,err}})$

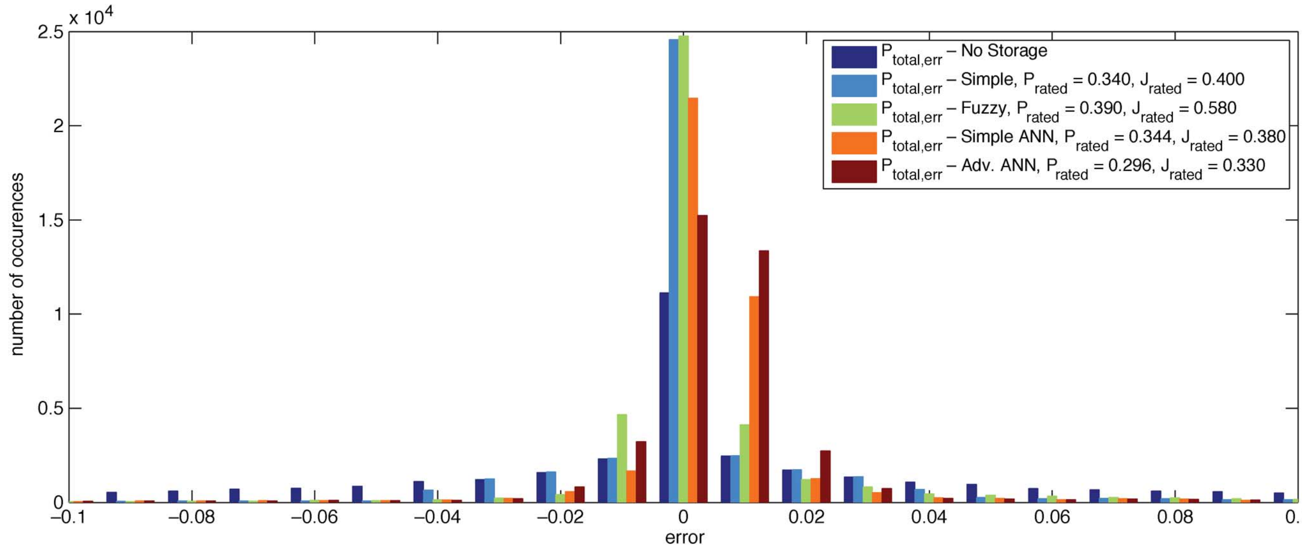

Fig. 10. $P_{\mathrm{total,err}}$ for all optimized systems.

TABLE III
OPTIMIZED RESULTS

	No ES	Simple	Fuzzy	Simple ANN	Adv. ANN
$Cost$	0	0.260	0.356	0.251	0.218
P_{rated}	NA	0.340	0.390	0.344	0.296
J_{rated}	NA	0.400	0.580	0.380	0.330
T	0.565	0.900	0.901	0.908	0.900
MAE	0.065	0.021	0.017	0.019	0.023
RMSE	0.113	0.058	0.048	0.056	0.062
max(E)	0.967	0.962	0.960	0.962	0.962
min(E)	-0.957	-0.634	-0.567	-0.634	-0.808
σ	0.113	0.058	0.047	0.056	0.062
R_{base}	0.176	0.173	0.172	0.172	0.173
C_{pen}	0.028	0.009	0.007	0.008	0.009
R_{total}	0.148	0.164	0.165	0.165	0.164

over 282 days of simulation time for all four of the controllers considered and their respective optimized P_{rated} and J_{rated}. The case of no energy storage is also shown. (Note that $P_{\mathrm{total,err}}$ for the no energy storage case is the same as $P_{\mathrm{wind,err}}$ for any case.) It is shown that the fuzzy and simple control-based systems have much greater occurrences of 0 error than using no energy storage. It is interesting to note that the ANN systems also have a high number of occurrences within the ± 0.04 band, but instead of being centered at 0, it is biased more toward 0.01. Operating at a slightly positive error (but still within the allowed band), results in a slight underproduction of power, which will save energy for more severe imbalances. This will also decrease the loss of energy in the system inefficiencies. This also gives some insight into how the fuzzy system may be redesigned for better performance.

VI. CONCLUSION

The variability of wind power limits its penetration and increases integration costs through increased reserve requirements. This paper demonstrates that through more effective control and coordination of energy storage systems, the wind farm output can be buffered to ensure that it produces the forecast amount of power within a tight tolerance (within 4% PU of the forecast power, 90% of the time). This allows utilities to decrease their spinning reserve requirements, as the energy storage system allows the combined wind farm and energy storage output to match the forecasted output with much greater reliability, resulting in decreased wind integration costs in terms of reserve requirements.

Four control strategies were considered. An optimization procedure was followed for each to determine the minimum cost energy storage system that could meet the target forecast with 4%, 90% of the time. For the simple and fuzzy controllers, a linear search of the energy storage system rated power and energy was conducted to find the lowest cost system. For the simple and advanced ANN controllers, a genetic algorithm was used to find a lowest cost system.

The results show that, assuming a simple control system and a 100-MW wind farm, the required energy storage system would cost approximately $26 million, and require 34 MW of power capability and 40 MWh of storage capacity. As a percentage of the wind farm capacity, this result is approximately consistent with other research findings [10], [11], [14] and commercial examples.[1]

The fuzzy controlled system required greater power and energy capacity, and resulted in a much higher cost system. The ANN controlled systems performed well, with the simple ANN performing comparably to the simple controller. The advanced variation (which considers SOC, unlike the simple ANN) performed significantly better than any other system, resulting in the lowest cost of $21.8 million for a 100-MW wind farm. This demonstrates that effective management of the system state of charge is essential.

However, it should be noted that the fuzzy controller memberships and rule set were not part of the optimization procedure. With optimization, the fuzzy performance could improve.

[1]The city of Presidio, TX, recently installed a 4-MW 32-MWh NaS battery system to provide city-wide backup power at a cost of approximately $25 M. This is comparable to our cost and sizing findings.

However, one of the attractive features of fuzzy controlled systems is that the control can be set up with a relatively simple, "common sense" based notion of reasonable operation of the system. Using an optimization procedure fuzzy memberships and rule sets risks losing the intuitive advantages of fuzzy controllers, while perhaps not gaining any advantage over a neural network.

It is also noted that although the advanced variation of the ANN resulted in the lowest cost system, its error metrics are less favorable than the other controllers although in many cases the difference is negligible. Looking at max(E), it is interesting to note that all systems experienced at some point an event where the forecasted output power was nearly 1 and the actual output was close to 0, and it did not vary much from system to system. However, for min(E), which represents a large event where the produced power greatly exceed the forecasted power, the simple, fuzzy, and simple ANN systems all were able to greatly reduce this imbalance, but less so with the advanced ANN. This is likely due to the advanced ANN-based system having the lowest J_{rated}, which would reduce its ability to suddenly absorb a large amount of energy.

The revenue and penalty calculations all show that the use of an energy storage system does not significantly affect the base revenue, but they do all greatly reduce the imbalance penalties, resulting in greater total revenue [31].

Lastly, an extended economic analysis comparing the savings in cost from reduced reserve requirements against the costs of the energy storage system is a good topic for future research. The methodology and results presented in this research can serve as critical inputs for this analysis.

Appendix

A penalty cost is subtracted from the base revenue when large imbalances in scheduled power production occur. The penalty scheme is based on [2] and applies a penalty for under or over production of power

$$C_{\text{pen}} = \begin{cases} 0, & |P_{\text{total,err}}| \le 0.04 \\ C_{\text{pen,under}}, & P_{\text{total,err}} > 0.04 \\ C_{\text{pen,over}}, & P_{\text{total,err}} < 0.04 \end{cases} \tag{13}$$

$$\begin{aligned} C_{\text{pen,under}} &= ((P_{\text{wind,FC}} - 0.04) - P_{\text{total}}) \\ &\quad \times (1.1 \cdot \text{price}_{\text{1mo,max}}) \end{aligned} \tag{14}$$

$$\begin{aligned} C_{\text{pen,over}} &= (P_{\text{total}} - (P_{\text{wind,FC}} + 0.04)) \\ &\quad \times (\text{price} - 0.9 \cdot \text{price}_{\text{1mo,min}}) \end{aligned} \tag{15}$$

where C_{pen} is the penalty cost applied, price is the current value of energy, $\text{price}_{\text{1mo,max}}$ is the maximum price over the last month, and $\text{price}_{\text{1mo,min}}$ is the minimum price over the last month. Note that the penalty for under production is much more severe than the penalty for over production. The penalty cost is subtracted from the base revenue to get the total revenue for each sample time

$$R_{\text{total}} = R_{\text{base}} - C_{\text{pen}} \tag{16}$$

$$R_{\text{base}} = P_{\text{total}} \cdot \text{price}. \tag{17}$$

Acknowledgment

The authors acknowledge the generous supply of large wind resource and wind farm data sets from Portland General Electric (PGE) and from Prof. S. Walker of the OSU Energy Resources Research Laboratory (ERRL), as well as wind pricing data from Powerdex, Inc. Beneficial discussions on the topics were also held with J. Pease and M. Hulse of the BPA, and C. Dieterle of PGE.

References

[1] Northwest's Wind Power Could Quadruple [Online]. Available: http://tinyurl.com/5tds3s

[2] A. Ingram, "Storage options and sizing for utility scale integration of wind energy plants," in *Proc. Int. Solar Energy Conf. 2005*, Orlando, FL, Aug. 2005, pp. 843–851.

[3] F. Baalbergen, P. Bauer, and J. Ferreira, "Energy storage and power management for typical 4q-load," *IEEE Trans. Ind. Electron.*, vol. 56, no. 5, pp. 1485–1498, May 2009.

[4] C. Abbey and G. Joos, "Sizing and power management strategies for battery storage integration into wind-diesel systems," in *Proc. Conf. IEEE Industrial Electronics (IECON)*, 2008.

[5] A. Shahirinia, S. Tafreshi, A. H. Gastaj, and A. Moghaddamjoo, "Optimal sizing of hybrid power system using genetic algorithm," in *Proc. Int. Conf. Future Power Systems*, Amsterdam, The Netherlands, 2005.

[6] R. Cardenas, R. Pena, G. Asher, and J. Clare, "Control strategies for enhanced power smoothing in wind energy systems using a flywheel driven by a vector-controlled induction machine," *IEEE Trans. Ind. Electron.*, vol. 48, no. 3, pp. 625–635, Jun. 2001.

[7] G. Cimuca, C. Saudemont, B. Robyns, and M. Radulescu, "Control and performance evaluation of a flywheel energy-storage system associated to a variable-speed wind generator," *IEEE Trans. Ind. Electron.*, vol. 53, no. 4, pp. 1074–1085, Jun. 2006.

[8] C. Abbey and G. Joos, "Supercapacitor energy storage for wind energy applications," *IEEE Trans. Ind. Appl.*, vol. 43, no. 3, pp. 769–776, May/Jun. 2007.

[9] B. Parkhideh, J. Zeng, S. Baek, S. Bhattacharya, M. Baran, and A. Huang, "Improved wind farm's power availability by battery energy storage systems: Modeling and control," in *Proc. IECON*, Orlando, FL, 2008, pp. 784–789.

[10] J. Zeng, B. Zhang, C. Mao, and Y. Wang, "Use of battery energy storage system to improve the power quality and stability of wind farms," in *Proc. PowerCon*, Oct. 2006, pp. 1–6.

[11] A. Shakib, E. Spahic, and G. Balzer, "Computation dimensioning of a sodium-sulphur battery as a backup of large wind farm," in *Proc. 16th PSCC*, Glasgow, Scotland, Jul. 2008.

[12] E. Spahic, G. Balzer, and A. Shakib, "The impact of the "wind farm-battery" unit on the power system stability and control," in *Proc. PowerTech*, Jul. 2007, pp. 485–490.

[13] S. Teleke, M. Baran, S. Bhattacharya, and A. Huang, "Optimal control of battery energy storage for wind farm dispatching," *IEEE Trans. Energy Convers.*, vol. 25, no. 3, pp. 787–794, Sep. 2010.

[14] S. Teleke, M. Baran, A. Huang, S. Bhattacharya, and L. Anderson, "Control strategies for battery energy storage for wind farm dispatching," *IEEE Trans. Energy Convers.* vol. 24, no. 3, pp. 725–732, Jun. 2009 [Online]. Available: http://dx.doi.org/10.1109/TEC.2009.2016000

[15] B. Roberts, "Capturing grid power," *IEEE Power Energy Mag.*, vol. 7, no. 4, pp. 32–41, Jul./Aug. 2009.

[16] J. Barton and D. Infield, "Energy storage and its use with intermittent renewable energy," *IEEE Trans. Energy Convers.*, vol. 19, no. 2, pp. 441–448, Jun. 2004.

[17] A. Price, "Technologies for energy storage present and future: Flow batteries," in *Proc. Power Engineering Society Summer Meeting*, Seattle, WA, 2000, pp. 1541–1545.

[18] H. Ibrahim and A. Llinca *et al.*, "Energy storage systems: Characteristics and comparisons," *Renewable and Sustainable Energy Rev.*, pp. 1221–1250, 2008.

[19] S. Schoenung and J. Eyer, Benefit and Cost Framework for Evaluating Modular Energy Storage Sandia National Laboratories, Tech. Rep., 2008.

[20] S. Schoenung and W. Hassenzahl, Long vs Short Term Energy Storage Technologies Analysis: A Life-Cycle Cost Study DOE Energy Systems Program, Tech. Rep..

[21] M. Khatibi and M. Jazaeri, "An analysis for increasing the penetration of renewable energies by optimal sizing of pumped-storage power plants," in *Proc. Electric Power Conf. (EPEC)*, Vancouver, BC, Canada, 2008, pp. 1–5.

[22] S. Lemofouet and A. Rufer, "A hybird energy storage system based on compressed air and supercapacitors with maximum efficiency point tracking (mept)," *IEEE Trans. Ind. Electron.*, vol. 53, no. 4, pp. 1105–1115, Aug. 2006.
[23] C. Brunetto and G. Tina, "Optimal hydrogen storage sizing for wind power plants in day ahead electricity market," *Renewable Power Generation*, vol. 1, no. 4, pp. 220–226, Dec. 2007.
[24] *Handbook of Electrochemistry*, C. G. Zoski, Ed. Amsterdam, The Netherlands: Elsevier BV, 2007.
[25] S. Chakraborty, M. Weiss, and M. G. Simoes, "Distributed intelligent energy management system for a single-phase high-frequency AC microgrid," *IEEE Trans. Ind. Electron.*, vol. 54, no. 1, pp. 97–109, Feb. 2007.
[26] J. Moreno, M. Ortuzar, and J. Dixon, "Energy-management system for a hybird electric vehicle, using ultracapacitors and neural networks," *IEEE Trans. Ind. Electron.*, vol. 53, no. 2, pp. 614–623, Apr. 2006.
[27] S. Lukic, J. Cao, R. Bansal, F. Rodriguez, and A. Emadi, "Energy storage systems for automotive applications," *IEEE Trans. Ind. Electron.*, vol. 55, no. 6, pp. 2258–2267, Jun. 2008.
[28] S. Zhou, L. Kang, G. Guo, Y. Zhang, J. Cao, and B. Cao, "The application of combinatorial optimization by genetic algorithm and neural network," in *Proc. Industrial Electronics and Applications*, Singapore, Jun. 2008, pp. 227–231.
[29] R. Rojas*, Neural Networks*. Berlin, Germany: Springer-Verlag, 1996.
[30] B. Wilamowski, "Neural network architectures and learning algorithms," *IEEE Ind. Electron. Mag.*, vol. 3, no. 4, pp. 56–63, Dec. 2009.
[31] H. Le and T. Nguyen, "Sizing energy storage systems for wind power firming: An analytical approach and a cost-benefit analysis," in *Proc. Power and Energy Society General Meeting*, Pittsburgh, PA, 2008, pp. 1–8.

Ted K. A. Brekken (M'06) received the B.S., M.S., and Ph.D. degrees from the University of Minnesota, in 1999, 2002, and 2005, respectively. He studied electric vehicle motor design at Postech in Pohang, South Korea, in 1999. He also studied wind turbine control at the Norwegian University of Science and Technology (NTNU) in Trondheim, Norway, in 2004–2005, on a Fulbright scholarship.

He is an Assistant Professor in Energy Systems at Oregon State University, Corvallis, OR. His research interests include control, power electronics, and electric drives, specifically digital control techniques applied to renewable energy systems. He is codirector of the Wallace Energy Systems and Renewables Facility (WESRF).

Dr. Brekken is a recipient of the NSF CAREER award.

Alex Yokochi received the B.S. and M.S. degrees from Southern Illinois University at Carbondale, and the Ph.D. degree from Texas A&M University, all in chemistry.

He is an Assistant Professor of chemical engineering at Oregon State University, Corvallis, OR. His research and teaching interests include the development of novel approaches to energy conversion and storage, and the development of functional materials with advanced properties through the development of nanocomposites.

Dr. Yokochi's work is supported by various state and federal agencies including Oregon BEST, ONAMI, the DoE, and the NSF through a CAREER award.

Annette von Jouanne (S'94–M'95–SM'00–F'09) received the Ph.D. degree in electrical engineering from Texas A&M University.

She has been a professor in the School of Electrical Engineering and Computer Science at Oregon State University (OSU), Corvallis, OR, since 1995. She also worked with Toshiba International Industrial Division at Texas A&M University. With a passion for renewables, she initiated the Wave Energy program at OSU in 1998, developing it into a national multidisciplinary program. She is also Codirecting the Wallace Energy Systems & Renewables Facility (WESRF).

Dr. von Jouanne has received national recognition for her research and teaching, and she is a Registered Professional Engineer as well as a National Academy of Engineering "Celebrated Woman Engineer."

Zuan Z. Yen received the Bachelors and MS degrees in electrical engineering with an emphasis on energy systems from Oregon State University, in 2007 and 2009, respectively.

He currently works for the Hydroelectric Design Center, Army Corps of Engineers, Portland, OR, as an Electrical Engineer. His work areas include power systems study, SCADA systems, protective relays, generation control, arc flash hazard analysis, and optimizing hydroelectric power plants.

Hannes Max Hapke (SM'04–M'10) received a prediploma from the University of Stuttgart, Germany, in 2006, and the M.S. degree from Oregon State University, in 2009.

He is a trainee at Vestas Wind Systems A/S, Aarhus, Denmark. He joined Vestas Global Research in 2009 and focused on energy storage research and wind power grid code compliance projects in the Vestas Power Plant R&D Department. Since Spring 2010, Hannes is also involved in a 2MW turbine development project for the Indian market. In May 2010, he will join the Product Management Department of Vestas Technology R&D.

Douglas A. Halamay (S'02–M'05–SM'08) received the BSEE degree (*summa cum laude*) with an emphasis in power from Gonzaga University, in 2005. He is a graduate student in energy systems at Oregon State University, Corvallis, OR.

After working for three years as a systems engineer on the P-8A Poseidon at Boeing Integrated Defense Systems, Renton, WA, he returned to graduate school to focus on power systems and renewable energy integration.